

Leader neurons in leaky integrate and fire neural network simulations

Cyrille ZBINDEN

Département de physique théorique

Université de Genève

CH-1211 Genève 4

Switzerland

E-mail: cyrille.zbinden@unige.ch

November 16, 2018

Abstract

In this paper, we highlight the topological properties of leader neurons whose existence is an experimental fact.

Several experimental studies show the existence of leader neurons in population bursts of 2D living neural networks [1, 2]. A leader neuron is, basically, a neuron which fires at the beginning of a burst (respectively network spike) more often than we expect by looking at its whole mean neural activity. This means that leader neurons have some burst triggering power beyond a simple statistical effect. In this study, we characterize these leader neuron properties. This naturally leads us to simulate neural 2D networks. To build our simulations, we choose the leaky integrate and fire (IIF) neuron model [3,4], which allows fast simulations [5, 6].

Our IIF model has got stable leader neurons in the burst population that we simulate. These leader neurons are excitatory neurons and have a low membrane potential firing threshold. Except for these two first properties, the conditions required for a neuron to be a leader neuron are difficult to identify and seem to depend on several parameters involved in the simulations themselves. However, a detailed linear analysis shows a trend of the properties required for a neuron to be a leader neuron. Our main finding is: A leader neuron sends a signal to many excitatory neurons as well as to a few inhibitory neurons and a leader neuron receives only a few signals from other excitatory neurons.

Our linear analysis exhibits five essential properties for leader neurons with relative importance. This means that considering a given neural network with a fixed mean number of connections per neuron, our analysis gives us a way of predicting which neuron can be a good leader neuron and which cannot. Our prediction formula gives us a good statistical prediction even if, considering a single given neuron, the success rate does not reach hundred percent.

Contents

Abstract	1
1 Introduction	3
2 The simulations	4
2.1 Building the simulations	4
2.2 Values of parameters and simulation choices	7
3 General appearance of the simulations	8
3.1 General appearance	8
3.2 Definitions	9
3.2.1 Definition of bursts and their triggers	9
3.2.2 Leaders	11
3.2.3 Mutual Information	11
4 Results	12
4.1 About the parameters and some statistics	12
4.2 Existence of leaders	12
4.3 Leader properties	14
4.3.1 Some facts about the leader properties	14
4.3.2 Finding the leader properties	16
4.4 First to fire neurons	20
5 Conclusion	22
Acknowledgments	23
Bibliography	23

1 Introduction

Disassociated *in vitro* rat brain neuron cultures show, under a variety of experimental contexts, a spontaneous electrical activity. This activity manifests itself by a rapid succession of ignitions of a large fraction of neurons named collective bursts (or network spikes) [7–10]. This bursting activity can be measured, for example, by multi-electrode array methods [1, 2, 11] or by fluorescence [12]. The study of the initiators of these bursts is one of the conceptual problems underlying the spontaneous electrical activity. A recent study [1] showed that some “first to fire” cells exist. Later [2], through a detailed analysis of data obtained by the multi-electrode array methods, established that some cells are triggering bursts beyond a simple statistical effect of being the first. These particular cells are called *leaders*. The analysis [2] indicates that the long term dynamics of the leaders is relatively robust, evolving with a half-life of about one day. [2] also shows that these leaders are not only the main initiators of bursts, but, the burst itself carries traces (or hints) indicating which of the leaders has initiated the burst. In this respect, one can view the culture as an amplifier of the signal emitted by the leaders.

It is clear that the scenario described above calls for a theoretical explanation. One of the ways pursued is the one of (bootstrap) percolation in random networks [13] which gives insights into the spread of the initial ignition and distinguishes between localized and de-localized spreading. In this picture, the burst itself is viewed as the “giant component” of the percolation process, and this picture is verified from many different angles [12].

In this paper, we address the delicate question of what makes a neuron a leader. Is it stimulation? Activity threshold? Special connectivity properties of the network? The natural way of reaching this aim theoretically is to simulate a random neural network. Our results show that leadership is an effect of a combination of several ingredients which can be quantified by a simple relation between several natural parameters of the neuron. We obtain these results by a simple model of a randomly connected network with the usual leaky integrate and fire [3] mechanism for ignition of neurons. This well known model [4] is tested in numerical event-based simulations that provides, in principle, unbiased simulations [14]. This model only takes into account simple properties of neurons (integrate and fire) [5, 6] but it suffices to reproduce basically all the findings of [2]. Thus we trade realism for conceptual simplicity, but in this kind of investigations the complexity comes from the neural network itself and not from the neuron model.

The results of our simulations can be presented as follows: to each neuron one can assign a leadership score and neurons with the highest scores are leaders. It turns out that leaders can be characterized as being excitatory neurons and having a low membrane potential firing threshold. Apart from these two first properties, the conditions required for a neuron to be a leader are difficult to identify and depend on several parameters involved in the simulations themselves. Indeed, a detailed linear analysis shows a trend of the properties required for a neuron to be a leader. The main finding of this paper is a formula for the leadership score that exhibits five essential properties for leaders with relative importance. This formula gives a very good statistical prediction. Therefore, we can conclude that leadership is a random effect, and that leaders are formed naturally from a balanced combination of inputs, outputs, their local neighborhood and their own properties. Basically a leader sends a signal to a lot of excitatory neurons as well as to a few inhibitory neurons and a leader receives only a few signals from other excitatory neurons.

2 The simulations

In this section we explain how we construct our leaky integrate and fire simulations and which kind of parameters we use.

2.1 Building the simulations

A single neuron is already a complex biological object. But, basically, neurons are electrically excitable cells that are composed of a soma (cell body), a dendritic tree and an axon. Dendrites and axons connect to each other (through synapses) to create a neural network. Thus, to make a model, we can, for example, choose a geometry and some rules that produce the rule of connection between neurons [15] or construct a random neural network with a fix mean number of connections per neuron.

Our simulations are built as follows. First we construct a matrix of synaptic weights W that represents a random neural network of $N \in \mathbb{N}$ neurons where N is a parameter and $\sqrt{N} \in \mathbb{N}$ as so we can consider that the neurons are placed on a grid $\{(x, y) \in \mathbb{N}^2 \mid x, y \leq \sqrt{N}\} \subset \mathbb{R}^2$ with periodic boundary conditions. In the Euclidean geometry of \mathbb{R}^2 , we consider that every neuron n ($n = 1, 2, \dots, N$) is a circle of radius $r \in \mathbb{R}_+$ (equivalent to the spatial extension of the dendrites). Each axon has a length $\ell \in \mathbb{R}_+$, approximately Gaussian distributed (with probability density function close¹ to $f(\ell, L) = \frac{1}{\lambda\sqrt{2\pi}}e^{-\frac{(\ell-L)^2}{2\lambda^2}}$ where $L \in \mathbb{R}_+$ is the mean axon length and $\lambda = \frac{1}{3}\min\left(L - 1, \frac{2}{3}\sqrt{N} - L\right)$ is the standard deviation (and $1 < L < \frac{2}{3}\sqrt{N}$). In our simulations, the neuron spatial parameters are the dendrite size r and the mean axon length L . To every axon, we also associate a direction (respectively an angle) $\theta \in [0, 2\pi)$ uniformly distributed (with probability density function $g(\theta) = \frac{1}{2\pi}$). Figure 1 illustrates the network geometry.

To construct the matrix $W \in \mathbb{M}_N(\mathbb{R})$, we proceed as follows: If the axon (with finite length ℓ , without width and angle θ (respectively direction)) of the neuron m ($m = 1, \dots, N$) intersects the circle (dendrites) of the neuron $n \neq m$ ($n = 1, \dots, N$) then the connection exists (*i.e.* $W_{nm} \neq 0$), otherwise $W_{nm} = 0$. The biological knowledge tells us that the connection between neurons is oriented (electrical impulses move from axons to dendrites). Thus we have a non-symmetric matrix of synaptic weights W representing the neural network.

A fix parameter $w \in \mathbb{R}_+$ named the synaptic weight is the value we give to W_{nm} when the connection exists (*i.e.* $W_{nm} \neq 0$). Note that, in reality, some neurons are inhibitors. For these, we use a negative synaptic weight $-w \in \mathbb{R}_-$. In our simulations the proportion $r \in [0, 1]$ of inhibitory neurons is also a parameter.

To simplify the terminology, if $W_{nm} \neq 0$, we will say that the neuron n is the son of the neuron m and the neuron m is the father of the neuron n . One given neuron can have more than

¹Negative axon lengths are not allowed and we impose a maximum length of $\frac{2}{3}\sqrt{N}$ for each axon. With this last condition, no axon can cover all the network in any direction. The rationale for this choice is that, in the experiments [2], probably no axon covers all the test tube in a given direction.

one father and more than one son. Of course, a given neuron can be both, father and son of another neuron.

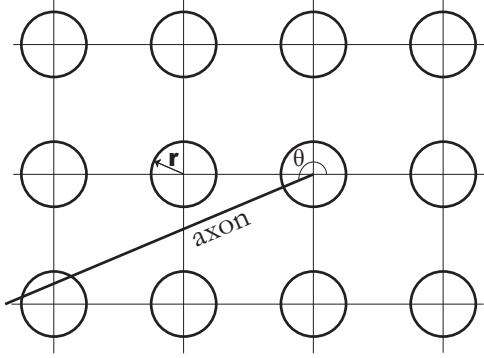


Figure 1: A 3×4 neurons rectangle. Each neuron is a circle with a radius $r \in \mathbb{R}_+$ (dendrites), in this figure $r < 1$. The axon of one of the neurons is drawn. We see that this neuron is connected to the neuron on the left of the bottom row. Note that the axon direction is given by $\theta \in [0, 2\pi)$. Note also that if $r \geq 1$, unlike in this figure, then we automatically have nearest neighbour connections.

Once the matrix of synaptic weights is constructed we assign two real values to each neuron n : V_n^* the membrane potential firing threshold and $V_n(t)$ the membrane potential which depends on the time $t \in \mathbb{R}_+$. Without loss of generality, we can consider that the membrane potential² oscillates roughly between 0 and $\langle V^* \rangle = 1$ (where $\langle V^* \rangle$ is the mean of all the neuron membrane potential firing thresholds). The time evolution of the membrane potential $V_n(t)$ is computed using the leaky integrate and fire [3] neuron model.

The dynamics is the following, every neuron n (respectively every membrane potential $V_n(t)$) which integrates the electrical signal it receives from the other neurons is able to fire (when $V_n(t) > V_n^*$) and then sends a signal to the other neurons. Just after firing the membrane potential is reset to 0. The membrane potential also decreases with a leaky time τ (loss of memory).

More precisely, the membrane potential evolution equation of the neuron n is the evolution equation of a leaky integrate and fire neuron model [3]

$$V_n(t + dt) = \underbrace{V_n(t)e^{-\frac{dt}{\tau}}}_{\text{Loss of memory}} \underbrace{(1 - \chi_n[V_n(t)])}_{\text{Reset after firing}} + \underbrace{\sum_{m=1}^N W_{nm} \chi_m \left[V_m \left(t - \frac{d_{nm}}{v} \right) \right]}_{\text{Connections}} + \underbrace{B_{t,n} \cdot \Omega_{t,n}}_{\text{Noise}} \quad (1)$$

where

- dt is the infinitesimal time step,
- $\tau \in \mathbb{R}_+$ is the leaky time (or characteristic time of the membrane [3]),
- $\chi_n[V_n(t)]$ is, for the neuron n , the indicator function of the set of potentials bigger or equal to V_n^* . Namely, $\chi_n[V_n(t)] = 1$ whenever $V_n(t) \geq V_n^*$ and $\chi_n[V_n(t)] = 0$ otherwise. The distribution of all the characteristic membrane potential firing threshold is approximately Gaussian with a probability density function close to $h(V^*) = \frac{1}{\Delta V^* \sqrt{2\pi}} e^{-\frac{(V^*-1)^2}{2\Delta V^{*2}}}$ where ΔV^* , the standard deviation, is a parameter,

²We know that the membrane potential oscillates more or less between -70 and -50 mV [3]. But to simplify, we will approximately scale the membrane potential between 0 and 1.

- $d_{mn} = d_{nm}$ is the distance between the neuron n and the neuron m . In the experiments related in [2], one finds a 2D density of about $2000 \frac{\text{cells}}{\text{mm}^2}$. This leads us here to fix the metric scale in our simulations: If we observe an expected mean number of neurons of 2000 neurons inside the grid square, we assume that this square measures 1 mm^2 . Nevertheless, we can also measure the distance in an arbitrary unit given by the expected number of neurons in a row but we need the metric scale to compare our signal propagation velocity to the experimental one,
- v is the propagation velocity of the signal in the neural network,
- $B_{t,n}$ is, for each time t and each neuron n , a Gaussian random variable with mean $\sigma > 0$ and standard deviation $\frac{\sigma}{3}$. Roughly speaking $B_{t,n} \sim \mathcal{N}(\sigma, \frac{\sigma}{3})$ for all n and for all $t > 0$. To generate this Gaussian noise, we use a Box-Muller transform,
- $\Omega_{t,n}$ is a Markovian exponential clock with a mean rate ω . For most t , one has $\Omega_{t,n} = 0$, but sometimes $\Omega_{t,n} = 1$. More precisely, the distribution of the time intervals Δt of the continuous set t where $\Omega_{t,n} = 0$ follows the exponential distribution $\frac{1}{\omega} e^{-\frac{\Delta t}{\omega}}$ (ω is the mean value). Finally, it means that $B_{t,n} \cdot \Omega_{t,n}$ is a noise $B_{t,n}$ which acts on the membrane potential of neuron n only when the exponential clock $\Omega_{t,n}$ rings.

By looking at (1), we see that, in principle, we can compute every membrane potential all the time. But it is not useful and too complicated to compute every membrane potential continuously. Choosing a fixed time step $\delta t > 0$ also introduces some problems like synchronized events and systematic errors [16]. In the program, made in Perl, we compute the membrane potential only when an event happens³. At this time, we check if the neuron fires or not. So, in the program, we store the events to find out the next membrane potential to update. In other words, our simulations (1) are event-based simulations. The firing time of neurons is not discretized but computed event per event at the machine precision level. This way of doing provides, in principle, unbiased simulations [14].

Note that if “every” neuron fires at (almost) the same time (this may happen in a burst) then all the membrane potentials are reset to 0 at the same time; the neurons are synchronized. To avoid that this situation occurs too often, when we initialize a sequence, we give to each neuron n a membrane potential in $[0, V_n^*)$ (uniformly distributed). Note that we reinitiate a sequence each time a burst is too long, so it is possible that during a simulation the neurons get synchronized.

Note also that if the mean exponential clock rate ω is too small relatively to the leaky time τ , it does not really matter which kind of distribution we use for the noise $B_{t,n}$. This means that if $\omega \ll \tau$ then we can use $B_{t,n} = \sigma$ for all t and for all n as the noise distribution $B_{t,n}$ and the result of the simulations remains the same.

³Here, by event we mean the moment when a neuron receives a signal from another neuron or when a neuron receives some noise (*i.e.* the Markovian exponential clock $\Omega_{t,n}$ rings).

2.2 Values of parameters and simulation choices

The parameters are fixed in a way to observe activity like the one observed in the experiments [2] when we restrict the observation to sixty neurons. This section provide a list of the order of magnitude of the parameters used in (1). Note that the reader can find almost all the information in [17].

- We made simulations for different sizes $N \in \mathbb{N}$. But beyond $N \sim 4$ it does not affect the presence of bursts and leaders. This means that we already get a leader when we consider only four neurons.
- In fact fixing the dendrites size r , the mean axon length L and the axons length distribution fix the distribution function for the sons (out-degree) and the mean number of connections per neuron (noted $\langle \text{connections/neuron} \rangle$). Remark that the number of sons per neuron distribution looks like the axons length distribution while the number of fathers per neuron distribution is always approximately Gaussian distributed (data not shown). Note also that the geometry we choosed for our simulations induces that the successful pre-burst shows locality, like the one observed by the authors in [2]. Finally in most of our simulations, we chose $r = 0.85$ and $L = 7$, then $\langle \text{connections/neuron} \rangle \cong 11$.
- The synaptic weight w is surely a function of the neuron and of the time (the neuron's learning). As soon as we choose mean number of connections per neuron and considering the kind of neural activity we want, we can fix w . We use $w \sim \frac{1}{10}$. Note that if $w \cong \langle V^* \rangle = 1$ (where $\langle V^* \rangle$ is the mean of all the neuron membrane potential firing thresholds) then all neurons are too strongly correlated and if $w = 0$ then all neurons are independent.
- For the inhibitory proportion r , the choice of $r = 0.2$ is reasonable. Depending on the neural culture type, the inhibitory cells proportion can change approximately from 20% to 30% (see [12]).
- In our simulations, the leaky time τ is about 100 ms. Note that the order of magnitude is the correct one [18]. To be exact we compute with $\tau = 0.1$ s, this means that the used time unit is the second.
- The propagation speed v in a neural network is between 50 and 100 $\frac{\text{mm}}{\text{s}}$, see [17]. In our case, v should be replaced by the propagation speed in the axon which is bigger. However, we have decided to use this range throughout.
- The standard deviation of the membrane potential firing threshold ΔV^* is also a parameter. We used $0 \leq \Delta V^* \leq 0.2 \langle V^* \rangle$, which guarantees that neurons are quit similar and still the membrane potentials do not get synchronized too often.
- For the exponential clock rate we use ω between 0.001 and 0.01 s.
- The mean noise σ is determined by the kind of neural activity we want to have (observe). If there is too much noise then we loose the locality in the successful pre-burst because we

have a lot of uncorrelated activities. Note that the mean membrane potential (without connection) $\bar{V} = \lim_{T \rightarrow \infty} \frac{1}{T} \int_0^T V(\tilde{t}) d\tilde{t}$ is about⁴ $\frac{\tau\sigma}{\omega}$. We want the mean membrane potential \bar{V} to be high enough to get some neural activity due to the noise. But we also want that $\bar{V} + w < \langle V^* \rangle$, so that one spike does not necessarily create a burst.

One might think that to keep the neural activity one can vary the values ω and σ keeping the ratio $\frac{\sigma}{\omega}$ constant because the mean membrane potential \bar{V} is about $\frac{\tau\sigma}{\omega}$. But to preserve the neural activity, the mean membrane potential \bar{V} is not that relevant. However it is necessary to keep constant the mean time the membrane potential of neurons need to reach the value V^* . From this point of view the relation between σ , ω and w is a first passage time problem. Note also that if the value of the mean membrane potential \bar{V} is too low then there is no neural activity due to the noise (this means no neural activity at all). To conclude, even if the exact value of the mean membrane potential \bar{V} is not fundamental, this value must not be too far from the mean of all neurons membrane potential firing threshold $\langle V^* \rangle$ (see [3]).

The parameters N , r , L , ΔV^* and r are the neural network parameters and the parameters τ , v , w , σ and ω are the dynamical parameters.

	Neural network parameters	Dynamical parameters
Known	$r \cong 20\%$ (inhibitory proportion) r, L , (mean number of connections)	$\tau \cong 100$ ms (leaky time) $v \cong 100 \frac{\text{mm}}{\text{s}}$ (propagation speed)
To be set	N (computing-memory) ΔV^* (firing threshold standard deviation)	$\langle V^* \rangle - \bar{V} > w > 0$ (synaptic weight) σ, ω (noise parameters)

Table 1: Known and unknown parameters of the simulations. The unknown parameters will be set in Section 4.1.

3 General appearance of the simulations and some definitions

In this section we show what is the product of our simulations and we give the definitions of what we call leader neuron, according to [2].

3.1 General appearance

Like in the experiments [1, 2, 10], we want to look at the neural activity. The product of our simulations consists of a list of ordered spikes times. For each spike i , the list gives us t_i , the time of the i^{th} spike, and n_i , the neuron that fired. Then, considering only the spike chronology, we analyze the “spike sequence” of a subset (or all) neurons of our simulations.

⁴The mean membrane potential charge due to the noise is $\sigma + \sigma e^{-\frac{w}{\tau}} + \sigma e^{-2\frac{w}{\tau}} + \dots = \frac{\sigma}{1 - e^{-\frac{w}{\tau}}} \cong \frac{\tau\sigma}{\omega}$ if $\frac{w}{\tau}$ is small.

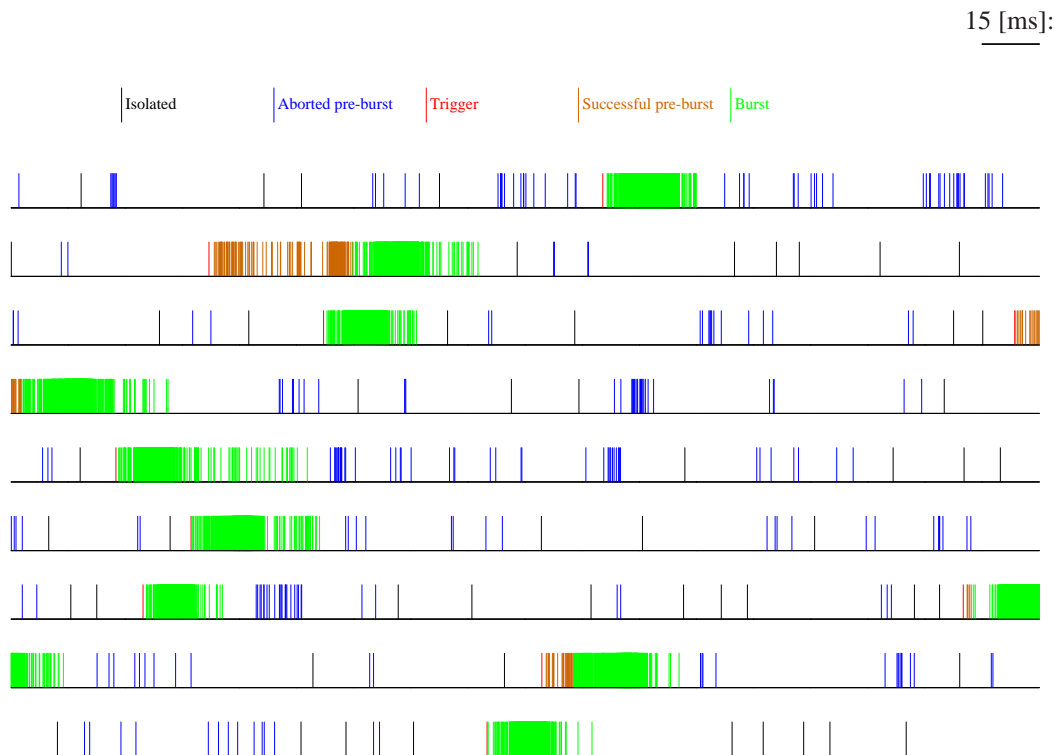


Figure 2: Picture of the temporal evolution of a simulation for the whole neural activity with the parameters: $N = 900$, $r = 0.85$, $L = 7$, $r = 0.2$, $\Delta V^* = 0.05$, $v = 5 \frac{1}{\text{ms}}$, $w = 0.1$, $\tau = 100$ ms, $\sigma = 0.008$, $\omega = 0.001$ s, $n_{\text{burst}} = 500$, $\delta t_{\text{burst}} = 15$ ms and $\delta t_{\text{isolated}} = 5$ ms. The color code, that gives a representation of the different definitions explained in the following section, is the following: **Isolated spike**, **aborted pre-burst**, **trigger**, **successful pre-burst**, and **burst**.

3.2 Definitions

Figure 2 represents a part of a simulation and leads us to define sequences in the simulations. This section is roughly the same than [2, Section 2.3]. Precisely we will define mathematically what we call a burst and a leader and we will also explain what we call mutual information. In order to make the present paper comparable to [2], we adhere strictly to the same definitions. So the reader who read [2] or knows these definitions can skip this part and move directly to the next section.

3.2.1 Definition of bursts and their triggers

First we divide all the spikes of our list into four classes: *burst*, *successful pre-burst*, *aborted pre-burst*, *isolated spike*, and each spike belonging to one and only one class. The precise definitions are given below, but basically a spike is in a burst if it is in a group of many spikes that follow each other closely. If a spike is not in a burst it can be in a successful pre-burst or aborted

pre-burst. But it must be anyway is in a sequence of spikes that are close enough in time so that communication between them is still possible. The distinction between successful or aborted pre-burst depends on whether the spike sequence is eventually followed by a burst or not. Finally, all other spikes are isolated.

More precisely, we use three parameters, n_{burst} , δt_{burst} , and $\delta t_{\text{isolated}}$. We first look for interspike gaps of length at least $\delta t_{\text{isolated}}$, and we divide the set of all spikes into disjoint subsets \mathcal{R}_k of consecutive spikes, where k is a running index. The \mathcal{R}_k have the property that if (the spike) i and $i + 1$ are in \mathcal{R}_k then $t_{i+1} - t_i \leq \delta t_{\text{isolated}}$, while if $i \in \mathcal{R}_k$ and $i + 1 \in \mathcal{R}_{k+1}$ then $t_{i+1} - t_i > \delta t_{\text{isolated}}$. The rationale is that if the interspike gap is so large that the spike $i + 1$ is due to noise and not to the axon signaling of the precedent (in time) spike i (i.e. $t_{i+1} - t_i > \delta t_{\text{isolated}}$ then the spikes belong to separate subsets).

We now want to further divide each \mathcal{R}_k into the burst itself, characterized by a high density of spikes, and its precursor which immediately precedes it in time but has a lower density. Each of the \mathcal{R}_k contains at least one spike, but may contain many. In each \mathcal{R}_k we first look for a spike that is followed by at least $n_{\text{burst}} - 1$ spikes in \mathcal{R}_k within a lapse of time δt_{burst} . Denoting this spike's index by $i_* = i_*(k)$, this is the first index in \mathcal{R}_k with the property:

$$t_{i_*+n_{\text{burst}}-1} - t_{i_*} < \delta t_{\text{burst}} . \quad (2)$$

If the condition (2) is met then we subdivide \mathcal{R}_k into two disjoint sets at i_* : $\mathcal{R}_k = \mathcal{P}_k \cup \mathcal{B}_k$ (\mathcal{P}_k can be empty). The index i_* up to the last index in \mathcal{R}_k make up the burst \mathcal{B}_k .

If the condition (2) is never met in \mathcal{R}_k , then the set \mathcal{R}_k is not subdivided. This is called an *aborted pre-burst* if it has more than one spike and is an *isolated spike* otherwise.

For these k where such an i_* can be found, we check if it is also the first spike in \mathcal{R}_k . If so, this burst is an *immediate burst* that has no successful pre-burst, so that $\mathcal{R}_k = \mathcal{B}_k$. For all the other bursts we divide $\mathcal{R}_k = \mathcal{P}_k \cup \mathcal{B}_k$ where \mathcal{P}_k are the index $i \in \mathcal{R}_k$ with $i < i_*$, and \mathcal{B}_k are the others. The letter \mathcal{P} refers to successful pre-bursts and \mathcal{B} refers to bursts.

Between bursts the neural activity is much lower, and we label these periods as *quiet*. Each quiet period, denoted \mathcal{Q}_b , for a running index b , is actually a concatenation of consecutive \mathcal{R}_k 's that did not contain a burst in the earlier stage, or else an empty set. We now renumber the set of index as follows

$$\{1, \dots, M\} = \mathcal{Q}_1 \cup \mathcal{P}_1 \cup \mathcal{B}_1 \cup \mathcal{Q}_2 \cup \mathcal{P}_2 \cup \mathcal{B}_2 \cup \dots ,$$

with \mathcal{B}_b the b 'th burst, \mathcal{P}_b the corresponding successful pre-burst (if it exists else \mathcal{P}_b is empty) and \mathcal{Q}_b the corresponding quiet phase. We define the *trigger* of burst b as the neuron n_{i_b} , where i_b is the number of the first spike in \mathcal{P}_b (resp. \mathcal{B}_b if \mathcal{P}_b is empty like for an immediate burst).

N	Analyzed neurons	n_{burst}	δt_{burst} [ms]	$\delta t_{\text{isolated}}$
900	60 900	20 > 100	15	$\frac{2}{3} \frac{\sqrt{N}}{v}$

Table 2: Burst detection parameters.

The parameters n_{burst} , δt_{burst} , and $\delta t_{\text{isolated}}$ that we used for $N = 900$ are shown in Table 2. Note that these parameters can easily be adapted for other values of the number of neurons N .

Remark also that the time parameters $\delta t_{\text{isolated}}$ and δt_{burst} have to be smaller than the characteristic time of the membrane τ . The rationale for these choices are: Firstly, to cross the distance of the biggest possible axon $\frac{2}{3}\sqrt{N}$, the signal, at the velocity v , needs a time of $\frac{2}{3}\frac{\sqrt{N}}{v}$. This computation gives us the order of $\delta t_{\text{isolated}}$. This means that only the signaling velocity is taken into account to compute $\delta t_{\text{isolated}}$. Secondly, even in a burst, the neural activity is not regular, so to balance this effect we need δt_{burst} to be high enough. Finally, for n_{burst} we want it high enough to guarantee that a burst includes many neurons.

3.2.2 Leaders

For every successful pre-burst, aborted pre-burst or immediate burst, the neuron which fires first is called the *trigger*. Since we are interested in their special rôle, we first need to make sure that triggers are not just neurons with high neural activity, which are statistically more often the first ones to fire. The following discussion will exhibit that leaders are over-proportionally more often triggers.

To qualify a neuron as a leader, we require that a trigger's probability to lead bursts should be significantly higher than its probability to fire. Let M be the total number of bursts in a simulation. For each neuron n , we define a_n as the number of times that neuron n has spiked during the simulation. Now, let us consider a spike, and term by q_n the probability⁵ that neuron n has fired that spike: $q_n = a_n / \sum_{n'} a_{n'}$. The probability for the neuron n to be a spurious, or random trigger F times in M bursts is given approximately⁶ by the binomial distribution $P_n(F)$:

$$\binom{M}{F} q_n^F (1 - q_n)^{M-F}. \quad (3)$$

In the limit of large M and reasonable q_n this distribution is approximated by a Gaussian of mean Mq_n and variance $Mq_n(1 - q_n)$. On the other hand, we denote by f_n the actual number of bursts that neuron n leads (note that $\sum_n f_n = M$).

Thus we have a scale on which to test triggering. We define α_n , a “leadership score”, and decide that a neuron is a *leader* if it scores at least 3 standard deviations above the natural expectation value. The criterion for leadership of neuron n is therefore

$$\alpha_n = \frac{f_n - Mq_n}{\sqrt{Mq_n(1 - q_n)}} > 3. \quad (4)$$

Because we expect $\alpha \sim \mathcal{N}(0, 1)$ to be Gaussian, (4) corresponds to a p-value of 0.001.

3.2.3 Mutual Information

We estimate the mutual information of two neurons (pair of neurons) in a series of time intervals based on empirical probabilities, according to [19]. Using the division (of time) into aborted

⁵unbiased estimator of the considered probability

⁶It would be exactly the binomial distribution if all the spikes were independent. All the spikes are certainly not independent because neurons are connected. So the binomial distribution is not the correct one but gives a good enough approximation (see [15]).

pre-burst, successful pre-burst and burst intervals, we define a firing event in a given interval as $h = 0, 1$, where 0 stands for no spike and 1 stands for at least one spike. We denote by $N_n(h)$ the number of times neuron n had an event h in a series of N_{int} intervals⁷. The probability assigned to the event h is thus⁵ $p_n(h) = N_n(h)/N_{\text{int}}$. The number of joint events in which neuron n had an event h_1 and neuron n' had an event h_2 is given by $N_{n,n'}(h_1, h_2)$. The joint probability of events h_1, h_2 for neurons n, n' is then given by⁵ $p_{n,n'}(h_1, h_2) = N_{n,n'}(h_1, h_2)/N_{\text{int}}$. The mutual information between two neurons is then given by

$$I_{n,n'} = \sum_{h_1, h_2 \in \{0,1\}} p_{n,n'}(h_1, h_2) \cdot \log \frac{p_{n,n'}(h_1, h_2)}{p_n(h_1)p_{n'}(h_2)}.$$

Note that the mutual information between two neurons is 0 if the two neurons fire independently and is $\ln 2$ if the two neurons fire always together (see [20]). These two extreme values give us the variation scale of the mutual information for a pair of neurons.

4 Results

In this section we explain our results. We prove that our simulations have stable leaders and we identify the topological properties of these leaders. An analysis of the first to fire neurons exhibits that the leader properties we find are the correct ones.

4.1 About the parameters and some statistics

The next step consists in analyzing our simulations knowing that our results will be more consistent if we span as many parameters as possible. However, our goal is not to obtain a transition phase diagram [21], so we are not going to vary all parameters (most of the them were fixed in Section 2.2 through Table 1). Up to now we stayed unclear about some parameters, including dynamical parameters like w , σ and ω . So we still have to find (and fix) a range for the parameters ΔV^* , w , σ and ω in a way to obtain “reasonable” simulations⁸ which involves distinguishing bursts, successful pre-bursts and quiet periods. One of the best ways to do that mathematically is to look at the time interspike distribution and compare with the experimental one (data not shown, see [15]). The analysis of the membrane potential profile and the time length distribution are also possible in the simulations (see [15]).

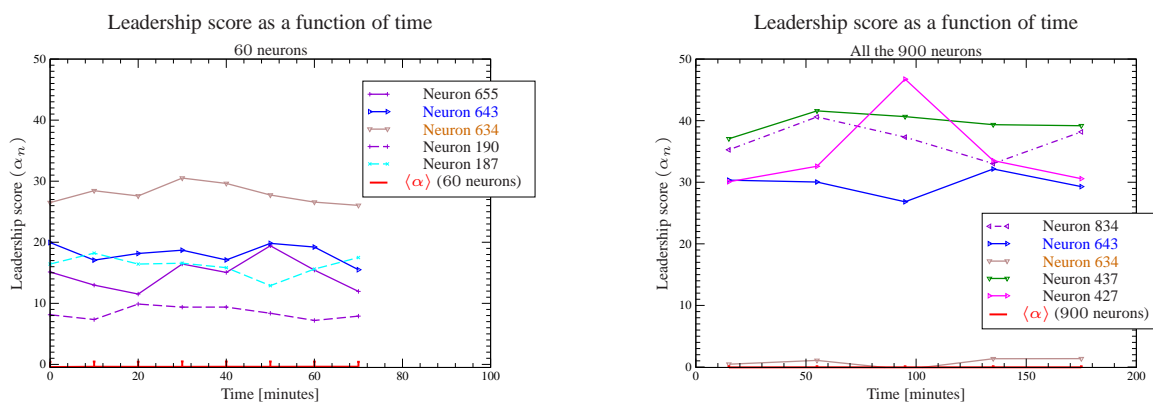
4.2 Existence of leaders

In Section 3.2.2, we defined, for every neuron n a leadership score α_n (see (4)) that compares the triggering frequency to the leadership expected frequency (compute with respect to the neural activity frequency). Figures 3 show the leadership score as a function of the time for a few

⁷Note that $N_{\text{int}} = M$ for the burst intervals and $N_{\text{int}} \leq M$ for the successful pre-burst intervals.

⁸Here by “reasonable” simulations, we mean to observe a neural activity more or less like the one in Figure 2 but without a precise predicting spike timing [22, 23].

neurons. In these figures we see that our simulations have leaders. Note that this result is very robust. We mean that the choice of the used parameters in simulations is not important. As soon as we use “reasonable” parameters, our simulations have leaders. This is still true when we only look at a few neurons instead of all them (Figure 3a). Even more, we can change the axons length distribution and the simulations still have stable leaders. Note also that even a network with a uniform probability of connections⁹ shows bursts and leaders but, in this case, we do not observe any spatial locality.



(a) The leadership score when we look at only 60 neurons like in [2]. We see that we have leaders and even very good ones. We also see that the average leadership score $\langle \alpha \rangle$ is about 0. Note that in this graph, each point represents 600 seconds of simulation that contains more than 2500 bursts. Remark that the **best leader** among 60 neurons is not necessarily a leader while we consider all the neurons (see Figure 3b). In the restricted case, the neurons detected as leaders can be first to fire neurons (see Section 4.4).

(b) The leadership score when we consider all the 900 neurons. We can say that these neurons are the “true” best leaders of the simulation. Note also that, luckily, **one** of the best leaders was in the 60 selected neurons. But even when it is not the case, when we consider only 60 neurons, some neurons show very good leadership scores. On this graph, each point represents about 2000 seconds of simulation that contains more than 8800 bursts.

Figure 3: Leadership score of a few neurons for the simulation shown in Figures 2. Note that the leadership score depends on the number of neurons considered for the analysis (see neuron 634, 643 and Section 4.4).

In our simulations, with $N > 400$ about 5% to 10% of the neurons have a mean leadership score (4) bigger than the threshold 3 when we consider all the neurons. While considering only 60 neurons, about 15% neurons have a mean leadership score bigger than the threshold 3. Also note that even if the leadership score can fluctuate during the simulations, its mean value stays stable (*i.e.* its standard deviation is small). Of course, the leader ratio decreases when the mean noise σ increases. This fact is logical because in a too noisy neural activity it becomes more difficult to identify the trigger of each burst. Note also that it seems that when ΔV^* (standard deviation of the membrane potential firing threshold) is between 0.05 and 0.1 the leader ratio seems maximal (data not shown).

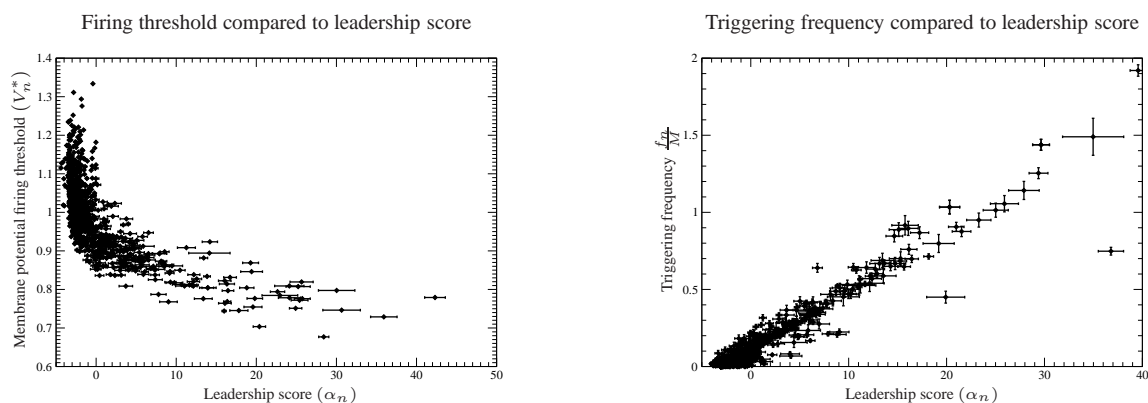
⁹This means a network that is not build with the kind of geometry showed in Figure 1.

In the experiments [2], one electrode captures in general the spike signal of several neurons [2, Figure 1a]. But, in our simulations, up to this point we considered each neuron separately, as if one electrode measures only one neuron. Remark that the leadership score of a group of neurons also reach the value 3 for some groups [15].

At this point, our simulations reproduce basically all the findings of [2] (presence of leaders, signature of bursts, force of leaders,...) see [15]. The advantage of simulations is that we have access to a lot of details that we did not have access to in the experiments and we can analyze the topology of the network to find out the properties of leaders.

4.3 Leader properties

4.3.1 Some facts about the leader properties



(a) The membrane potential firing threshold (V_n^*) compared to the leadership score (α_n). We see that good leaders have a low membrane potential firing threshold ($\langle V_n^* \rangle = 1$). Parameters: $N = 900$, $r = 0.85$, $L = 7$, $r = 0.2$, $\Delta V^* = 0.1$, $v = 5 \frac{1}{\text{ms}}$, $w = 0.1$, $\tau = 100$ ms, $\sigma = 0.008$, $\omega = 0.001$ s, $n_{\text{burst}} = 100$, $\delta t_{\text{burst}} = 15$ ms and $\delta t_{\text{isolated}} = 5$ ms.

(b) The triggering frequency (f_n/M) compared to the leadership score (α_n). These two things are proportional. Parameters: $N = 900$, $r = 0.85$, $L = 7$, $r = 0.2$, $\Delta V^* = 0.05$, $v = 5 \frac{1}{\text{ms}}$, $w = 0.1$, $\tau = 100$ ms, $\sigma = 0.008$, $\omega = 0.001$ s, $n_{\text{burst}} = 100$, $\delta t_{\text{burst}} = 15$ ms and $\delta t_{\text{isolated}} = 5$ ms.

Figure 4: Some properties of leaders for simulations with parameters close to the one we showed in Figure 2. Note that each point in these figures represents an average of the results for 5 simulations using the same neural network and the same parameters. Each simulation contains more than 10000 bursts and the simulated time was longer than 25 minutes.

In Figures 4 we see clearly that the leaders seem to have some special properties compared to the other neurons. More precisely, Figure 4a shows that good leaders typically have a low membrane potential firing threshold. This fact exhibits that to be a good leader, a neuron must have the property of firing early. But, this property is not the only one a neuron needs to have to be a leader. Indeed the best leader in Figure 4a is not the neuron with the lowest membrane potential firing threshold. Thus, another property of the leaders is easy to highlight: the leaders

are excitatory neurons¹⁰ (data not shown). In Figure 4b, we see that, like in [2], the better a leader is, the more bursts it triggers.

We can also have a look at the leadership score compared to the neural activity ratio of the neurons shown in Figure 5. Firstly, remember that to compute the leadership score we use the neural activity ratio q (see (4)). Secondly, look at Figure 5 and remark that there are as much leaders with a high neural activity ratio as leaders with a low neural activity ratio. So, clearly and as expected, for a given neuron there is no link between having a high leadership score and the neural activity ratio, even if a good leader triggers a lot of bursts (see Figure 4b).

Before trying to find more leader properties, we add more remarks about Figure 5. We note that there exist some neurons with a very high positive leadership score ($\alpha > 10$) but there is no neuron with a very low leadership score ($\alpha < -10$). We also note that if the standard deviation of the membrane potential firing threshold ΔV^* is 0 then most of the neurons have a neural activity ratio near $\bar{q} = \frac{1}{N}$ (in Figure 5 $\bar{q} = \frac{1}{900} \cong 0.11\%$ as expected).

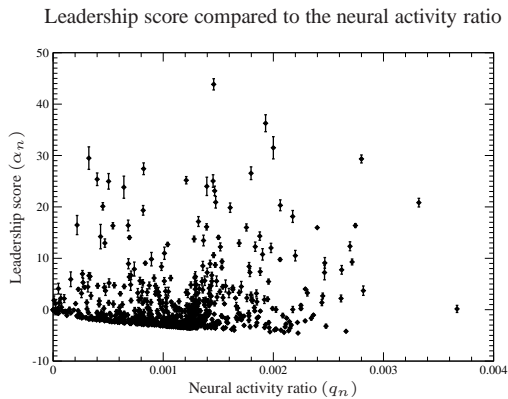


Figure 5: The leadership score (α) compared to the neural activity ratio (q). Note that, as before, each point in this figure represents an average of the results for 5 simulations using the same neural network. Parameters: $N = 900$, $r = 0.85$, $L = 7$, $r = 0.2$, $\Delta V^* = 0.1$, $v = 5 \frac{1}{\text{ms}}$, $\tau = 100 \text{ ms}$, $w = 0.1$, $\sigma = 0.008$, $\omega = 0.001 \text{ s}$, $n_{\text{burst}} = 100$, $\delta t_{\text{burst}} = 15 \text{ ms}$ and $\delta t_{\text{isolated}} = 5 \text{ ms}$.

Unfortunately, the other relations between a property and the leadership score that we tried to highlight did not exhibit an as good correlation as the relations showed in Figures 4. We also note another important fact: In the special case where we use a network with every membrane potential firing threshold fixed to $\langle V^* \rangle$ (*i.e.* $\Delta V^* = 0$) or/and without inhibitory neurons (*i.e.* $r = 0$), our simulations still have stable leaders. These two facts lead us to the following hypothesis: the properties of leaders are a non trivial combination of properties.

To find these properties, we perform the following experiment: We take a given network¹¹ and make several simulations with this network but change some of the dynamical parameters (τ ,

¹⁰Remark that in the special case where $\omega \ll \tau$, we rarely observed a few inhibitory neurons with a leadership score bigger than 3. This can happen only when these inhibitory neurons have a very low membrane potential firing threshold, a few excitatory fathers and a lot of inhibitory fathers. The reason is as follow, because $\omega \ll \tau$, the network gets synchronized after the first burst and these particular inhibitors have the faculty to fire even before the true trigger of the burst. Beside the type of their fathers implies a very low neural activity, so their leadership scores are potentially good. Note that the few top best leaders are always excitatory neurons.

¹¹This means that we choose N , r , L , p , ΔV^* , r and build a realization of a network (*i.e.* W and V_n^* are known for all n).

v , w , σ and ω) in a way of keeping a reasonable¹² simulation. Then, we compute the leadership score of each neuron and we do this for each simulation. As a result, we find that the best leader is not always the same even if most of the time a leader stays leader. Figure 6 illustrates this fact and this forces us to admit that the leader properties depend on the dynamical parameters. Nevertheless, we can probably find a trend of the properties of a typical leader by doing a linear least squares analysis for all our simulations. Indeed, in Figure 6 more than 90% of the leaders keep on being leaders and non leaders keep on being non leaders under the change of dynamical parameters.

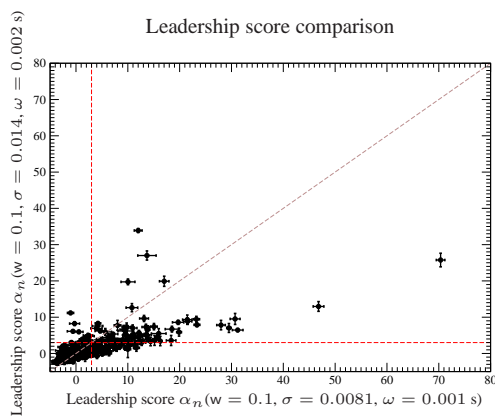


Figure 6: The leadership score of two different simulations using the same neural network. The **red dashed lines** separate leaders and non-leaders for both simulations. We observe that the best leader is not necessarily the same and some neurons are leaders with a set of parameters but are not leaders with the other set. We also observe that most of the time a good leader continues being a good leader in both simulations. Like for Figures 4, the error bars are computed by averaging over 5 simulations using the same network and dynamical parameters w , σ and ω . Common parameters: $N = 900$, $r = 0.85$, $L = 7$, $r = 0.2$, $\Delta V^* = 0.1$, $v = 5 \frac{1}{\text{ms}}$, $\tau = 100 \text{ ms}$, $n_{\text{burst}} = 100$, $\delta t_{\text{burst}} = 15 \text{ ms}$ and $\delta t_{\text{isolated}} = 5 \text{ ms}$.

Before going through this linear least squares analysis, note that in the experiments related in [2], the leaders change during the days spent *in vitro* with a typical life time of about one day (see [2, Figure 3a]). While, in the simulations, the leaders stay the same in a given network if we do not change the dynamical parameters of the simulation. So, one of the interesting facts in the simulations is that to change the leaders we do not need to change the network, some changes in the dynamical parameters are enough (we consider the synaptic weight w as a dynamical parameter).

4.3.2 Finding the leader properties

To find out the leader properties we do the following linear least square analysis. First, we build a vector $\vec{\alpha} = \{\alpha_n\}_{n=1, \dots, N}$ that contains the leadership score α_n of each neuron n of a given simulation. Then we construct a matrix $P = \{P_{ni}\}_{1 \leq n \leq N, 1 \leq i \leq 6}$ that contains all the neuron properties (excitatory or inhibitory neuron and membrane potential firing threshold) and all the

¹²Here by a reasonable simulation, we mean that we want to observe quiet periods, successful pre-bursts and bursts in a way to find leaders. Note that this range of reasonable parameters is quite large and the relation between the dynamical parameters is non trivial, see remark in Section 2.2 and Section 4.1.

connection properties at the first order¹³. More precisely: $P_{n1} = 1$ if the neuron n is an excitatory neuron and -1 otherwise. $P_{n2} = \frac{V_n^* - \langle V^* \rangle}{\Delta V^*}$ if $\Delta V^* > 0$ and 0 otherwise. P_{n3} is number of excitatory neurons connected to the axon of neuron n (this means the number of excitatory sons of the neuron n , see Section 2.1) and P_{n4} the number of inhibitory sons. Identically, P_{n5} is the number of excitatory fathers of the neuron n and P_{n6} the number of inhibitory fathers.

Our linear least square method, like in [24], consists in finding a vector $\vec{x} = \{x_i\}_{i=1,\dots,6}$ such that the euclidean norm

$$\|P\vec{x} - \vec{\alpha}\| \quad (5)$$

is minimized. This particular \vec{x} gives us the relations (at the linear order) between the first order properties¹⁴ of a neuron and its leadership score.

By repeating the calculation (5) for each of our simulations and averaging over all our simulations, we obtain the typical solution $\vec{x} = (1.22, -2.33, 0.13, -0.19, -0.13, 0)^T$. This means that a good prediction p_n for the leadership score α_n of the neuron n in a network is given by

$$p_n = 1.22 \cdot P_{n1} - 2.33 \cdot P_{n2} + 0.13 \cdot P_{n3} - 0.19 \cdot P_{n4} - 0.13 \cdot P_{n5}, \quad (6a)$$

$$\text{if } \Delta V^* > 0: \quad p_n = 1.22 \cdot \text{excitatory}_n - 2.33 \cdot \frac{V_n^* - \langle V^* \rangle}{\Delta V^*} + 0.13 \cdot \# \text{ excitatory sons}_n - 0.19 \cdot \# \text{ inhibitory sons}_n - 0.13 \cdot \# \text{ excitatory fathers}_n \quad (6b)$$

where ($\text{excitatory}_n =$) $P_{n1} = 1$ if the neuron n is an excitatory neuron and -1 otherwise, $P_{n2} = \frac{V_n^* - \langle V^* \rangle}{\Delta V^*}$ if $\Delta V^* > 0$ and 0 otherwise, P_{n3} ($= \# \text{ excitatory sons}_n$) is the number of excitatory sons (of neuron n), P_{n4} ($= \# \text{ inhibitory sons}_n$) is the number of inhibitory sons and P_{n5} ($= \# \text{ excitatory fathers}_n$) is the number of excitatory fathers.

Note also that (6) do not depend on the axons length distribution. Even more, by building a fully random network (without axons and dendrites, *i.e.* no particular geometry) and fixing only the mean number of connections per neuron, we obtain the same formula.

Precisely, equations (6) mean that a typical leader in our simulations is an excitatory neuron, that it has a low membrane potential firing threshold and that it has a lot of excitatory sons but a few inhibitory sons and a few excitatory fathers. Equations (6) in this exact form are valid for a mean number of connections per neuron of about eleven ($\langle \# \text{ connections/neuron} \rangle \cong 11$).

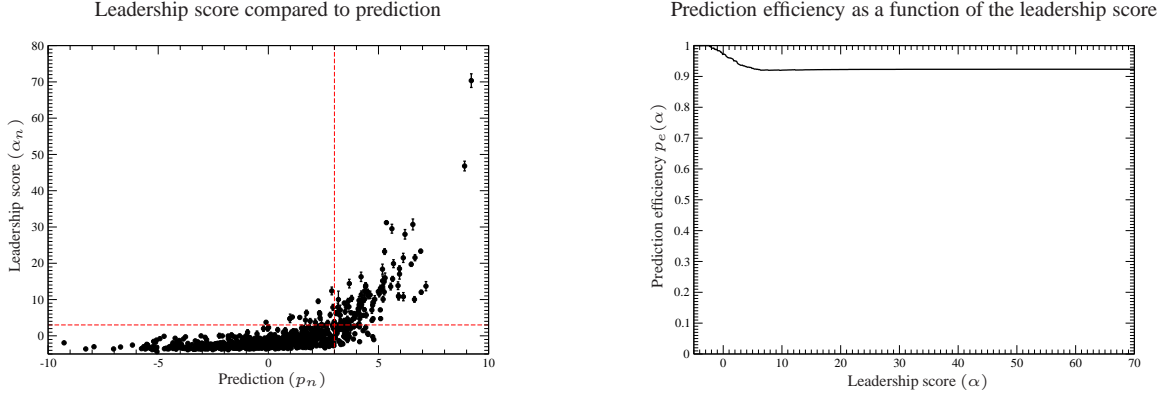
Now, considering a given neural network (that we did not use to obtain (6)) and using (6), we can predict, even before running our simulation which neuron will be a leader and which not. Figure 7a shows a typical prediction. Remark that this prediction is pretty reliable because: All the neurons with a prediction p_n lower than 0 are not leaders and all the neurons with a prediction p_n bigger than 6 are leaders ($\alpha_n > 3$). More precisely, Figure 7b shows the prediction efficiency¹⁵ p_e as a function of the leadership score α . In Figure 7b we can also remark that the prediction is correct for more than 90% of the neurons ($p_e(\alpha) > 0.9 \quad \forall \alpha$). This means that

¹³We call connection properties at the first order all the direct connections of the neuron in the network contained in the matrix of synaptic weights W (this means the number of sons and fathers (see Section 2.1)).

¹⁴We call first order properties all the neuron properties and all the connection properties at the first order.

¹⁵We call prediction efficiency the coefficient $p_e(\alpha) = \frac{\sum_{n|\alpha_n < \alpha} \text{correct prediction}_n}{\sum_{n|\alpha_n < \alpha} 1}$ where $\text{correct prediction}_n$ is 1 if the neuron n is a leader $\alpha_n > 3$ (respectively not a leader $\alpha_n \leq 3$) in the simulation and its prediction $p_n > 3$ (respectively $p_n \leq 3$), otherwise: $\text{correct prediction}_n = 0$.

Figure 7b shows that the trend of prediction is correct. Of course Figure 7b also shows that there are some mistakes in the predictions especially for prediction (p_n) between 0 and 6 (see Figure 7a). It is important to remember that the leaders are function of the dynamical parameters and our coefficients in (6) (which are only computed at the linear order) are not.



(a) The leadership score (α_n) compared to the prediction (p_n) for a particular simulation. The **red dashed lines** separate leaders and non-leaders for both the simulation and the prediction. As usual, the error bars of each point in this figure are computed using 5 simulations done with the same network and parameters.

(b) The prediction efficiency of Figure 7a. For each neuron n we attach a number, named correct prediction $_n$, which is 1 if the neuron n is a leader $\alpha_n > 3$ (respectively not a leader $\alpha_n \leq 3$) in the simulation and its prediction $p_n > 3$ (respectively $p_n \leq 3$), otherwise: correct prediction $_n = 0$. For each value of the leadership score α , we compute the prediction efficiency $p_e(\alpha) = \frac{\sum_{n|\alpha_n \leq \alpha} \text{correct prediction}_n}{\sum_{n|\alpha_n < \alpha} 1}$ which is plot as a function of the leadership score α .

Figure 7: Effectiveness of the prediction formula (6). Parameters: $N = 900$, $r = 0.85$, $L = 7$, $r = 0.2$, $\Delta V^* = 0.1$, $v = 5 \frac{1}{\text{ms}}$, $\tau = 100 \text{ ms}$, $w = 0.1$, $\sigma = 0.0081$, $\omega = 0.001 \text{ s}$, $n_{\text{burst}} = 100$, $\delta t_{\text{burst}} = 15 \text{ ms}$ and $\delta t_{\text{isolated}} = 5 \text{ ms}$.

Figure 8 shows the prediction efficiency¹⁵ as a function of the leadership score α . Most of the simulations presented in Figure 8 show that the trend of prediction of (6) is correct ($p_e(\alpha) \geq 0.9$, $\forall \alpha$). Precisely, for a range of simulations with different standard deviation of the membrane potential firing threshold (ΔV^*) (Figure 8 simulations **B**, **D**, **E** and **F**), for different mean noise (σ) and exponential clock rate (ω) (Figure 8 simulations **C** and **F**) the trend of prediction is correct. So by looking only at the simulations **B**, **C**, **D**, **E** and **F** of Figure 8, we can say that (6) give a pretty good prediction (even without adapting the coefficient of (6) with the dynamical parameters). But for the simulation **A** the trend of prediction is less good ($p_e(\alpha) \leq 0.9$, $\forall \alpha > 0$). The fact is the following, for the simulation **A**, the inhibitory proportion $r = 0$. This means that for simulation **A** we did not stay in the parameters range that we gave in Section 2.2 and that we used to find out (6). We can say that the fact that (6) does not give a very good trend of predictions for the simulation **A** is a kind of edge effect. With $\vec{x}_{r=0} = (-0.8927, -3.23, 0.07, \lambda_1, -0.02, \lambda_2)^T$ in (6) (where $\lambda_1, \lambda_2 \in \mathbb{R}$), we obtain a much better prediction for simulation **A** ($p_e(\alpha) \geq 0.92$, $\forall \alpha$). Remark that the first number (-0.8927)

(the coefficient of $P_{n1} = \text{excitatory}_n$) of $\vec{x}_{r=0}$ has no physical meaning because all neurons are excitatory neurons (if $r = 0$ then $P_{n1} = \text{excitatory}_n = 1 \forall n$). For the same reason λ_1, λ_2 in $\vec{x}_{r=0}$ can be any real number because P_{n4} (= # inhibitory son $_n$) and P_{n6} (= # inhibitory fathers $_n$) are always 0 if all neurons are excitatory neurons. All this means that the relative importance of the leader properties change by changing the parameters of the simulation but the trend in (6) is correct. The sign of each coefficient in (6) is robust (as soon as the coefficient has a physical meaning).

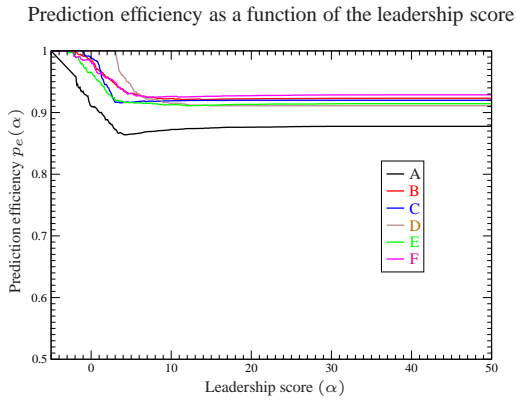


Figure 8: The prediction efficiency $p_e(\alpha) = \frac{\sum_{n|\alpha_n < \alpha} \text{correct prediction}_n}{\sum_{n|\alpha_n < \alpha} 1}$ as a function of the leadership score α for different simulations (see Figure 7b). **A)** $r = 0$, $w = 0.0666$, $\Delta V^* = 0.1$, $\sigma = 0.008$ and $\omega = 0.001$ s, **B)** $r = 0.2$, $w = 0.1$, $\Delta V^* = 0.05$, $\sigma = 0.008$ and $\omega = 0.001$ s, **C)** $r = 0.2$, $w = 0.1$, $\Delta V^* = 0.1$, $\sigma = 0.014$ and $\omega = 0.002$ s, **D)** $r = 0.2$, $w = 0.1$, $\Delta V^* = 0$, $\sigma = 0.008$ and $\omega = 0.001$ s, **E)** $r = 0.2$, $w = 0.1$, $\Delta V^* = 0.2$, $\sigma = 0.007$ and $\omega = 0.001$ s, **F)** $r = 0.2$, $w = 0.1$, $\Delta V^* = 0.1$, $\sigma = 0.008$ and $\omega = 0.001$ s, Common parameters: $N = 900$, $r = 0.85$, $L = 7$, $v = 5 \frac{1}{\text{ms}}$, $\tau = 100$ ms, $n_{\text{burst}} = 100$, $\delta t_{\text{burst}} = 15$ ms and $\delta t_{\text{isolated}} = 5$ ms.

We can also explain why we do not use a bigger matrix P . Considering a given neural network, we can extract a lot of different properties for all neurons n : the number of fathers, the number of sons, the number of fathers' fathers (second order property¹⁶), the number of loop order 2, 3, 4, 5 . . . in which the neuron n participates, . . . We can also reduce the network to an excitatory network and so on. We can as well try to improve our results by using a lot of tricks and/or cut off. But using the properties at the first order seem to be an easy and logical way of doing. Especially considering two facts: 1) A son will not necessarily fire after one of his fathers did, so what to say about the sons of this son? 2) The leadership score depends on the dynamical parameters. Taking that fact into account improves more the result than considering the second order properties in the network.

To conclude, (6) cannot be taken as a general law and (6) is only a good approximation of the leadership score in the range of parameters we chose in Section 2.2. However, we pretend that the signs in (6) are robust under the change of parameters. This means that our typical leader profile is the right one.

We pretend that even if (6) are computed on small scale simulations, the trend of the typical leader profile is the correct one. Even more we propose to use the following leader profile if the

¹⁶This means that we need to compute W^2 to extract this property.

mean number of connections per neuron vary

$$\text{if } r, \Delta V^* > 0: \quad p_n = \begin{aligned} & 1.22 \cdot \text{excitatory}_n - 2.33 \cdot \frac{V_n^* - \langle V^* \rangle}{\Delta V^*} + 1.14 \cdot \frac{\# \text{ excitatory sons}_n}{(1-r) \langle \# \text{ connections/neuron} \rangle} \\ & - 0.42 \cdot \frac{\# \text{ inhibitory sons}_n}{r \langle \# \text{ connections/neuron} \rangle} - 1.14 \cdot \frac{\# \text{ excitatory fathers}_n}{(1-r) \langle \# \text{ connections/neuron} \rangle}. \end{aligned} \quad (7)$$

This equation was computed knowing that in (6): $\langle \# \text{ connections/neuron} \rangle = 11$.

We have already explained in Section 4.2 that we observe leaders in our simulations as soon as we use reasonable parameters. Further more, considering a given simulation, we can store the neurons using the leadership score. After that, if we decide to remove some of the (best) leaders from the network and then run again our simulation we still observe leaders (as good as before). Finally, in a leaky integrate and fire neuron model there are leaders in the networks and the neurons which fit better with the typical leader profile are the leaders.

4.4 First to fire neurons

In this section we characterize the first to fire neurons. From this point, we will call first to fire neurons the neurons that fire in a short time after the trigger. This means that the first to fire neurons fire roughly in the successful pre-burst.

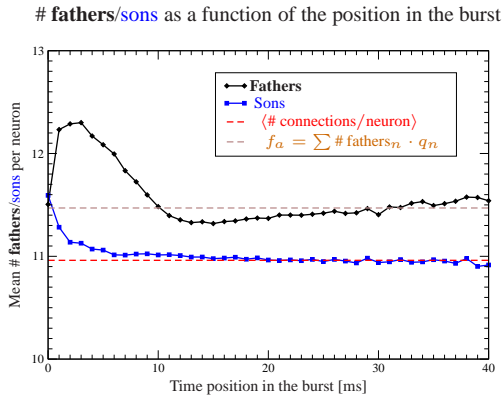


Figure 9: The mean number of **fathers/sons** per neuron as a function of the time position of a spike of this neuron in the burst. The time bin in which we average the number of **fathers/sons** per neuron is 1 ms. The time position 0 is reserved for the trigger of the burst. The mean number of connections per neuron in the network (noted $\langle \# \text{ connections/neuron} \rangle$) is about 11. The typical number of fathers of an active neuron f_a is about 11.5 (see (8) for definition). We obtained this figure by averaging over more than 35000 bursts. Parameters: $N = 900$, $r = 0.85$, $L = 7$, $r = 0.2$, $\Delta V^* = 0.05$, $v = 5 \frac{1}{\text{ms}}$, $w = 0.1$, $\tau = 100 \text{ ms}$, $\sigma = 0.008$, $\omega = 0.001 \text{ s}$, $n_{\text{burst}} = 150$, $\delta t_{\text{burst}} = 15 \text{ ms}$ and $\delta t_{\text{isolated}} = 5 \text{ ms}$.

Figure 9 shows the mean number of fathers (or sons) per neuron as a function of the time position of a spike of this neuron in the burst. To obtain Figure 9 we average over all the bursts of a given simulation without taking into account if the trigger of the burst was a leader or not. Nevertheless, when we look at the mean number of sons per trigger¹⁷ we remark that the trigger of the burst has, on average, more sons than their followers. This fact is consistent with our previous analysis. Remember that Figure 4b shows that leaders trigger more bursts than other neurons. This means that the trigger is, on average, a leader. Remember also that (6) tells that a leader has typically many excitatory sons (this means a lot of sons as well).

¹⁷The time position 0 in Figure 9 is reserved for the trigger of the burst.

Figure 9 also shows that the first to fire neurons have, on average, more sons than their followers and have, on average, less sons than the trigger. This means that very often several leaders are present in the successful pre-burst (this is linked with the triggering force of leaders, data not shown but see [15]). So the fact that first to fire neurons have typically a lot of sons is consistent with (6).

In Figure 9 the mean number of sons per neuron tends to the mean number of connections per neuron in the network. This means that, except for the trigger and the first to fire neurons, the mean number of sons per neuron for the neurons which fire during the burst itself is not relevant.

Figure 9 shows explicitly that the mean number of fathers per neuron of the first to fire neurons is higher than the mean number of connections per neuron in the network. This means that the first to fire neurons are characterized by a high number of fathers. This is consistent with the fact that neurons with a lot of fathers light up early in the burst, respectively in the successful pre-burst (see [25]). In fact neurons with a lot of fathers have a higher neural activity than neurons with a few fathers (data not shown). And again, this is consistent with [25] and Figure 9 which shows that active neurons in the burst are, on average, neurons with a lot of fathers (typically more fathers than the mean number of connections per neuron in the network).

In Figure 9 the mean number of fathers per neuron (unlike the mean number of sons) does not tend to the mean number of connections per neuron in the network but seems to increase again after the decay of the first to fire neurons. This is consistent with the following fact: in a burst, after a while, neurons are able to fire again (as soon as their membrane potentials are charged enough). And, of course, the neurons with a lot of fathers are able to fire again sooner than the others.

What about the mean number of fathers of the trigger? Figure 9 shows a tendency of the trigger to have more fathers than the mean number of connections per neuron. This last fact seems to contradict our predictions (6). But in Figure 9 the mean number of fathers of the trigger is approximately what we call the typical number of fathers of an active neuron f_a :

$$f_a = \sum_{n=1}^N \# \text{ fathers}_n \cdot q_n \quad (8)$$

where $\# \text{ fathers}_n$ is the number of fathers of neuron n and q_n is the neural activity ratio of neuron n . Figure 9 shows that (except for the first to fire) the mean number of fathers per neuron is about f_a the typical number of fathers of an active neuron and shows that the number of fathers of the typical trigger is not different from f_a . These two facts can explain the term concerning the number of fathers in (6), but still, we can think it contradicts (6).

To clarify this conflict, let us have a look at Figure 10. This figure shows, as Figure 9, the mean number of fathers (and sons) per neuron as a function of the time position of a spike of this neuron in the burst. In Figure 10 the standard deviation of the membrane potential firing threshold ΔV^* is much higher than the one in Figure 9. In Figure 10, we see that the number of sons of the trigger as well as the one of the first to fire neurons is higher than the mean number of connections per neuron in the network. And we see that the number of fathers of the trigger is lower than the mean number of connections per neuron in the network. But the number of fathers of the first to fire neurons is higher than the mean number of connections per neuron in

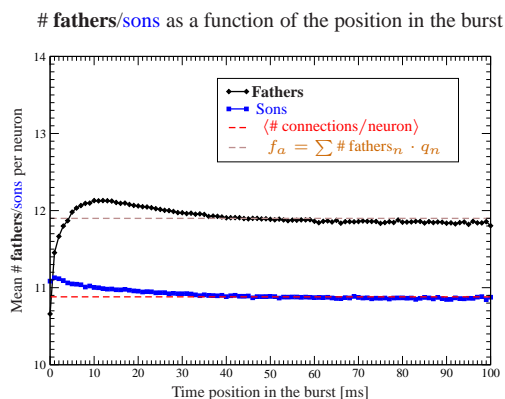


Figure 10: The mean number of **fathers/sons** per neuron as a function of the time position of a spike of this neuron in the burst. The time bin in which we average the number of **fathers/sons** per neuron is 1 ms. The time position 0 is reserved for the trigger of the burst. The mean number of connections per neuron in the network (noted $\langle \# \text{connections/neuron} \rangle$) is about 11. The typical number of fathers of an active neuron f_a is about 11.9 (see (8) for definition). We obtained this figure by averaging over more than 35000 bursts. Parameters: $N = 900$, $r = 0.85$, $L = 7$, $r = 0.2$, $\Delta V^* = 0.2$, $v = 5 \frac{1}{\text{ms}}$, $w = 0.1$, $\tau = 100 \text{ ms}$, $\sigma = 0.007$, $\omega = 0.001 \text{ s}$, $n_{\text{burst}} = 150$, $\delta t_{\text{burst}} = 15 \text{ ms}$ and $\delta t_{\text{isolated}} = 5 \text{ ms}$.

the network. This force us to conclude that the simulation shown in Figure 10 does not contradict (6). The reason for that is that the membrane potential firing threshold plays a more important rôle in this case.

We can also remark that in Figure 9 like in Figure 10, the mean number of fathers per neuron tends approximately to the typical number of fathers of an active neuron f_a while we look forward in time in the burst.

Now, let us clarify the observation of Figures 3 concerning the neurons 634 and 643. Neuron 643 is one of the best leaders of the simulation of Figure 3b while restricting the observation to 60 neurons only implies that neuron 634, which is not a leader (see Figure 3b), appears as a leader (see Figure 3a). The fact is that both neurons 634 and 643 have the profile of first to fire neurons (mean number of fathers close to the typical number of fathers of an active neuron). But the membrane potential firing threshold of the two neurons explain why only neuron 643 can be a leader: $V_{634}^* = 1.009$ and $V_{643}^* = 0.869$ ($\langle V^* \rangle = 1$ and $\Delta V = 0.05$). So while restricting the observation to 60 neurons only, it is possible that the first to fire neurons appear as leaders. In the experiments [2] it was impossible to distinguish between true leaders and first to fire neurons.

Finally we have a competition between two facts: To be a leader, a neuron needs to be able to fire early (in order to do that it must have a low membrane potential firing threshold and a lot of fathers) and to be a leader, a trigger must trigger more bursts than we expect. Typically a leader has a good triggering power (this means a lot of excitatory sons) and a relatively low neural activity ratio (this means less fathers than the typical number of fathers of an active neuron). That is the message of (6) (respectively (7)). Remember that (6) was obtained by averaging over simulations, so (6) express only a tendency of what kind of neurons the leaders are.

5 Conclusion

Experimental studies show the existence of leader neurons in population bursts of 2D living neural networks [1,2]. This leads naturally to a question: Do leaders also exist in neural network

simulations? In this study, we have proved that stable leaders exist in leaky integrate and fire neural network simulations.

In our simulations, we saw that leaders depend on the network but also on the dynamical parameters. Because the leaders mainly depend on the network and on the own properties of the neurons, we were able to find some important properties for these leaders. Firstly, they are excitatory neurons and have a low membrane potential firing threshold (ability of firing early). Secondly, they send a signal to a lot of excitatory neurons and to a few inhibitory neurons (triggering power). Finally, they receive only a few signal from other excitatory neurons (trigger more bursts than we expect by looking at the neural activity).

The study of more biological plausible models [5, 6] (like Hodgkin-Huxley) would be very interesting too and could probably also produce stable leaders. These models could probably be used to find out other leader properties.

Acknowledgments

I would like to thank Jean-Pierre Eckmann, my PhD advisor at the University of Geneva, Switzerland, for his continuous useful help along this study. This paper could not have been without the help of Elisha Moses, Weizmann Institute of Science, Israel. During all this research, I was supported by the Fonds National Suisse. Finally I would like to thank Sonia Iva Zbinden.

References

- [1] D. Eytan and S. Marom. Dynamics and effective topology underlying synchronization in networks of cortical neurons. *J. Neurosci.*, 26(33):8465–8476, 2006.
- [2] J.-P. Eckmann, S. Jacobi, S. Marom, E. Moses, and C. Zbinden. Leader neurons in population bursts of 2D living neural networks. *New J. Phys.*, 10(015011), 2008.
- [3] W. Gerstner and W. M. Kistler. *Spiking neuron models. Single neurons, populations, plasticity*. Cambridge University press, 2002.
- [4] B. Cessac. A discrete time neural network model with spiking neurons. Rigorous results on the spontaneous dynamics. *Journal of Mathematical Biology*, 56(3):311–345, 2008.
- [5] E. M. Izhikevich. Which model to use for cortical spiking neurons? *IEEE transactions on neural networks*, 15(5):1063–1070, 2004.
- [6] R. Naud and W. Gerstner. How good are neuron models? *Science*, 326:379–380, 2009.
- [7] A. Tschertter, M.O. Heuschkel, P. Renaud, and J. Streit. Spatiotemporal characterization of rhythmic activity in rat spinal cord slice cultures. *Eur J Neurosci*, 14(2):179–190, 2001.

-
- [8] E. Maeda, H.P. Robinson, and A. Kawana. The mechanisms of generation and propagation of synchronized bursting in developing networks of cortical neurons. *J Neurosci*, 15(10):6834–6845, 1995.
- [9] M.H. Droge, G.W. Gross, M.H. Hightower, and L.E. Czisny. Multielectrode analysis of coordinated, multisite, rhythmic bursting in cultured CNS monolayer networks. *J Neurosci*, 6(6):1583–1592, 1986.
- [10] D.A. Wagenaar, J. Pine, and S.M. Potter. An extremely rich repertoire of bursting patterns during the development of cortical cultures. *BMC Neurosci*, 7(11), 2006.
- [11] D.A. Wagenaar, J. Pine, and S.M. Potter. Searching for plasticity in dissociated cortical cultures on multi-electrode arrays. *J Neg Res BioMed*, 5(1):16, 2006.
- [12] J. Soriano, M. Rodriguez Martinez, T. Tlusty, and E. Moses. Development of input connections in neural cultures. *Proc Natl Acad Sci USA*, 105(37):13758–13763, 2008.
- [13] J.-P. Eckmann and T. Tlusty. Remarks on bootstrap percolation in metric networks. *J. Phys. A: Math. Theor*, 42(205004), 2009.
- [14] B. Cessac, O. Rochel, and T. Viéville. Introducing numerical bounds to event-based neural network simulation. *arXiv*, (0810.3992), 2008.
- [15] C. Zbinden. *Leader Neurons in Living Neural Networks and in Leaky Integrate and Fire Neuron Models*. PhD thesis, University of Geneva, 2010. <http://archive-ouverte.unige.ch/unige:5451>.
- [16] B. Cessac and M. Samuelides. From Neuron to Neural Network Dynamics. *EPJ Special Topics*, 142(1):7–88, 2007.
- [17] L. Gruendlinger, J.-P. Eckmann, O. Feinerman, J. Soriano, and E. Moses. The Physics of Living Neural Networks. *Physics reports*, 449:54–76, 2007.
- [18] E. Alvarez-Lacalle and E. Moses. Slow and fast waves in 1-D cultures of excitatory neurons. 2007.
- [19] J.-P. Eckmann, E. Moses, and D. Sergi. Entropy of dialogues creates coherent structures in e-Mail traffic. *PNAS*, 101(40):14333–14337, 2004.
- [20] N. Ay and A. Knauf. Maximizing multi-information. *Kybernetika*, 42(5):517–538, 2006.
- [21] R. Naud, N. Marcille, C. Clopath, and W. Gerstner. Firing patterns in the adaptive exponential integrate-and-fire model. *Biological Cybernetics*, 99:335–347, 2008.
- [22] R. Brette and W. Gerstner. Adaptive Exponential Integrate-and-Fire Model as an Effective Description of Neuronal Activity. *J Neurophysiol*, 94:3637–3642, 2005.

-
- [23] H.-R. Luscher R. Jolivet, A. Rauch and W. Gerstner. Predicting spike timing of neocortical pyramidal neurons by simple threshold models. *Journal of Computational Neuroscience*, 21:35–49, 2006.
- [24] J.H. Wilkinson and C. Reinsch. *Linear algebra*. Springer, 1971.
- [25] O. Cohen, A. Keselman, E. Moses, M. Rodriguez Martinez, J. Soriano, and T. Tlusty. Quorum percolation: More is different in living neural networks. *submitted*, 2009.